CrossMark

Influence of climate regime shift on the interdecadal change in tropical cyclone activity over the Pacific Basin during the middle to late 1990s

Chi-Cherng Hong[1] · Yi-Kai Wu[1,2] · Tim Li[3]

Abstract In this study, a new interpretation is proposed for the abrupt decrease in tropical cyclone (TC) activity in the western North Pacific (WNP) after the late 1990s. We hypothesize that this abrupt change constitutes a part of the phenomenon of interdecadal change in TC activity in the Pacific Basin, including the WNP, western South Pacific (WSP), and eastern North Pacific. Our analysis revealed that the climate-regime shift (CRS) in the Pacific during the middle to late 1990s resulted in a La Niña-like mean state, which was responsible for the interdecadal change in TC activity in the late 1990s. Analyses of the TC genesis potential index and numerical experiments revealed that the decline in TC activity in both the WNP and WSP was primarily attributable to the increase of vertical wind shear in the central Pacific due to the La Niña-like associated cold sea surface temperature (SST). Conversely, the La Niña-like associated warm SST in the western Pacific produced anomalous vertical transport of water vapor, increasing moisture levels in the mid-troposphere and TC activity in the western WNP. Furthermore, the CRS modified the mean TC genesis position and shifted the steering flow to the west, resulting in the increased frequency of TC landfalls in Taiwan, southeastern China, and northern Australia after the late 1990s.

✉ Chi-Cherng Hong
   cchong@utaipei.edu.tw; hong0202@gmail.com

[1] Department of Earth and Life, University of Taipei,
     1 Ai Kuo West Road, Taipei 10048, Taiwan

[2] Department of Earth Sciences, National Taiwan Normal
     University, Taipei, Taiwan

[3] IPRC/SOEST, University of Hawaii at Manoa, Honolulu,
     HI, USA

1 Introduction

The western North Pacific (WNP) constitutes part of the warm pool, where tropical cyclone (TC) genesis occurs the most frequently. TC activity in the WNP exhibits marked interannual and interdecadal fluctuation (Chan 2000; Chia and Ropelewski 2002; Wang and Chan 2002; Camargo and Sobel 2005; Chan 2005). For example, the frequency of TC genesis was unusually high in 1994, when 34 TCs formed; however, TCs numbered only 26 in 1995. Broadly, TC genesis frequency was high in the mid-1960s and mid-1990s, but relatively low in the 1980s and late 1990s (Liu and Chan 2013; Choi et al. 2015; He et al. 2015). Inter-annual variation in TC activity in the WNP is associated with large-scale circulation anomalies caused by the El Niño–Southern Oscillation (Li 2012) and the stratospheric quasi-biennial oscillation (Chan 2005; Liu and Chan 2013). Conversely, the strength and extent of the North Pacific subtropical high (NPSH) are the principal factors modifying the interdecadal variation in TC activity in the WNP (Chan 2005; Hsu et al. 2014).

The tropical Pacific underwent a basin-scale climate regime shift (CRS) during the middle to late 1990s (Hong et al. 2013). This CRS, which was characterized by a negative sea surface temperature anomaly (SSTA) in the equatorial eastern Pacific and a positive SSTA in both the tropical western Pacific and the entire subtropical Pacific, was accompanied by a pair of low-level atmospheric anticyclone and cyclone anomalies in the tropical western and eastern Pacific. The low-level anticyclone anomaly in the WNP facilitated the NPSH to extend westward, potentially

suppressing TC activity in the WNP (Chia and Ropelewski 2002; Liu and Chan 2013; Chan 2005).

Recent studies have identified a significant interdecadal decrease in TC activity in the WNP after the late 1990s (Liu and Chan 2013; Hsu et al. 2014; He et al. 2015). These studies attributed this reduction to increases in both the large-scale vertical shear and the 500-hPa geopotential height. Although the decline of TC activity in the WNP after the late 1990s has been investigated extensively, most previous studies have focused on the specific region of TC genesis in the WNP. Thus, it remains unclear whether this interdecadal change can be detected in adjacent genesis regions, such as the western South Pacific (WSP) and eastern North Pacific (ENP). Additionally, the physical processes underlying the interdecadal increase in TC genesis frequency in the northwestern part of the WNP remain obscure (He et al. 2015). The simultaneous occurrence of both the abrupt change in TC activity and the CRS in the Pacific during the middle to late 1990s suggests that they were related. Therefore, this study considered the role of the basin scale CRS in the abrupt change in TC activity in the late 1990s. We hypothesized that the abrupt decrease in TC activity in the WNP was associated with the greater phenomenon of interdecadal change in TC activity in the Pacific Basin. This includes changes in TC activity in the WNP and the WSP, and a westward shift of the mean TC genesis position in the WNP and the ENP. In addition, the large-scale factors causing the interdecadal change in TC activity in the Pacific were related to La Niña-like background (mean) changes, which ultimately resulted from the Pacific CRS during the middle to late 1990s.

2 Data and methodology

Data from the International Best Track Archive for Climate Stewardship (Knapp et al. 2010) for the period 1960–2012 were used to analyze the change in TC frequency. This data set was obtained from the Regional Specialized Meteorological Center of the World Meteorological Organization and other agencies (e.g., the Joint Typhoon Warning Center and the Japan Meteorology Agency). Because tropical depression wind speeds in the Southern Hemisphere were not available until 1980, TC activity in the WSP was analyzed using data starting from that year. In addition, the typhoon season (October–April) covers two calendar years in the Southern Hemisphere. Therefore, the annual mean number of TCs within this region was based on the period from July to the following June. Monthly atmospheric data sets based on the NCEP/NCAR Reanalysis I (Kalnay et al. 1996) and monthly SST fields from the Met Office Hadley Centre sea ice and sea surface temperature data sets

(Rayner et al. 2003) were employed for diagnosing the large-scale circulation anomalies.

A regime-shift index (RSI) (Rodionov 2004) was used to detect the specific time of the CRS. Here, a cutoff length of 10 years was applied for CRS diagnosis, and only values of the RSI that exceeded the 0.05 significance level were considered. A sensitivity test of the CRS was performed by calculating the RSI with cutoff lengths of 8 and 12 years (not shown). The test indicated that the abrupt change in TC activity in the Pacific in the late 1990s was robust.

3 Abrupt change in TC activity in the Pacific Basin in the late 1990s

3.1 TC genesis frequency

Figure 1 illustrates a time series of the annual TC count in various genesis regions of the Pacific. The number of TCs in the WNP demonstrated clear interdecadal variation, with active periods in 1965–1975 and 1985–1995, and inactive periods in 1976–1984 and 1998–2012. The RSI calculation shows that during the 53-year period (1960–2012), three significant and abrupt changes occurred in the number of TCs in 1968, 1988, and 1998. Among these years, the abrupt decrease in TC activity in 1998 was particularly pronounced. The average annual number of TCs was 29 during the active period of 1984–1997; however, it decreased to 24 during the inactive period of 1998–2011.

The time series of TC activity in the WSP illustrates that TC genesis frequency was high in the 1990s and low in the 2000s. The RSI calculation indicates that the number of TCs decreased abruptly and significantly in 1999. Because the typhoon season (October–April) covers two calendar years in the Southern Hemisphere, this change in TC activity can be considered concurrent with the decrease in TC activity in the WNP in 1998 on the interdecadal time scale. Further examination showed that the abrupt changes in TC activity in the WNP and the WSP during the late 1990s were caused primarily by a change in TC activity during the typhoon season (i.e., June to October in the Northern Hemisphere, and November to the following April in the Southern Hemisphere). TC activity during the nontyphoon season did not exhibit any significant interdecadal change. The sensitivity of the RSI for 1998–1999 was further tested using cutoff lengths of 8 and 12 years, and the results demonstrated that the change point for the period of approximately 1998–1999 was robust. Considering this change point, the active period of TC genesis, 1986–1997, was denoted as IP1, and the inactive period, 1998–2009, as IP2.

The TC activity in the ENP reveals that TC genesis frequency was high during 1980–1994, however, it did not show significant change after 1995. Weak TCs (i.e., tropical
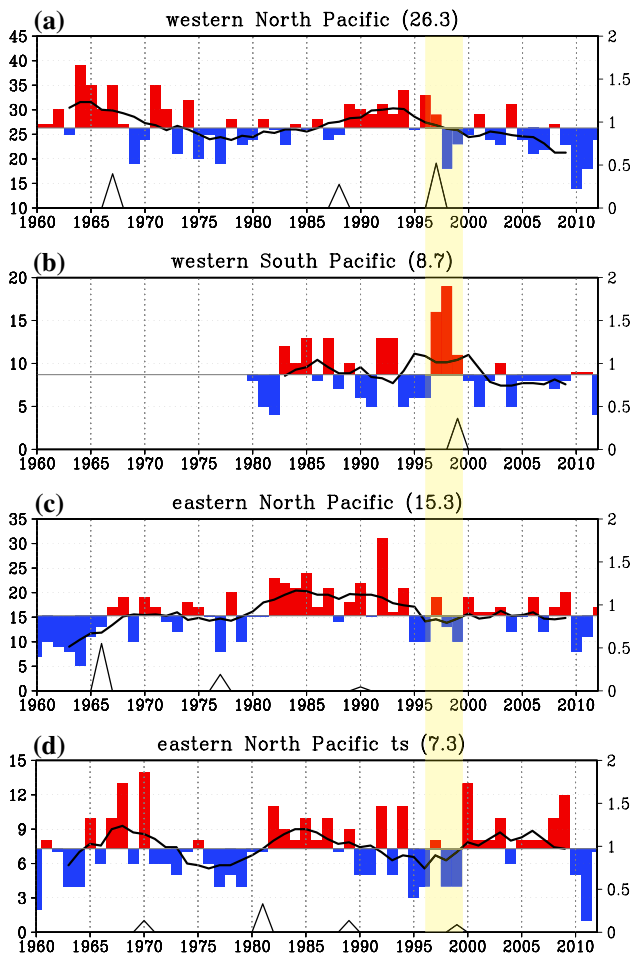
Fig. 1 **a** Time series of annual (*filled line*) and 7-year running mean (*black line*) of the number of TCs in the WNP during 1960–2012. The *thick black line* at the *bottom* shows the regime-shift index (RSI) (Rodionov 2004) with 10-year cutoff length. Only the RSI exceeding 95 % confidence is plotted. The *horizontal line* denotes the climatological mean (1960–2012) of the number of TCs. **b**, **c** Same as in (**a**) except for the TC-genesis regions in the western South Pacific (WSP) and eastern North Pacific (ENP), respectively. **d** is the same as (**c**), except for the weak TC (maximum sustain wind, 34–63 knots). The *numbers in the brackets* indicate the climatological annual mean numbers of TC-genesis. The *yellow vertical bar* indicates the period of the abrupt change in TC activity in the Pacific Basin during middle to late 1990s

storms, having a maximum sustained wind speed of 34–63 knots) exhibited an interdecadal increase (Fig. 1d), whereas strong TCs (having a maximum sustained wind speed of >63 knots) exhibited an interdecadal decrease after the late 1990s (i.e., the result of Fig. 1c subtracted from that of Fig. 1d). This reversed interdecadal change is similar to that described by Lupo (2011). Because the interdecadal increase of weak TCs was offset by the interdecadal decrease of strong TCs, the total annual mean number of TCs in the ENP did not show a significant interdecadal change in the late 1990s.
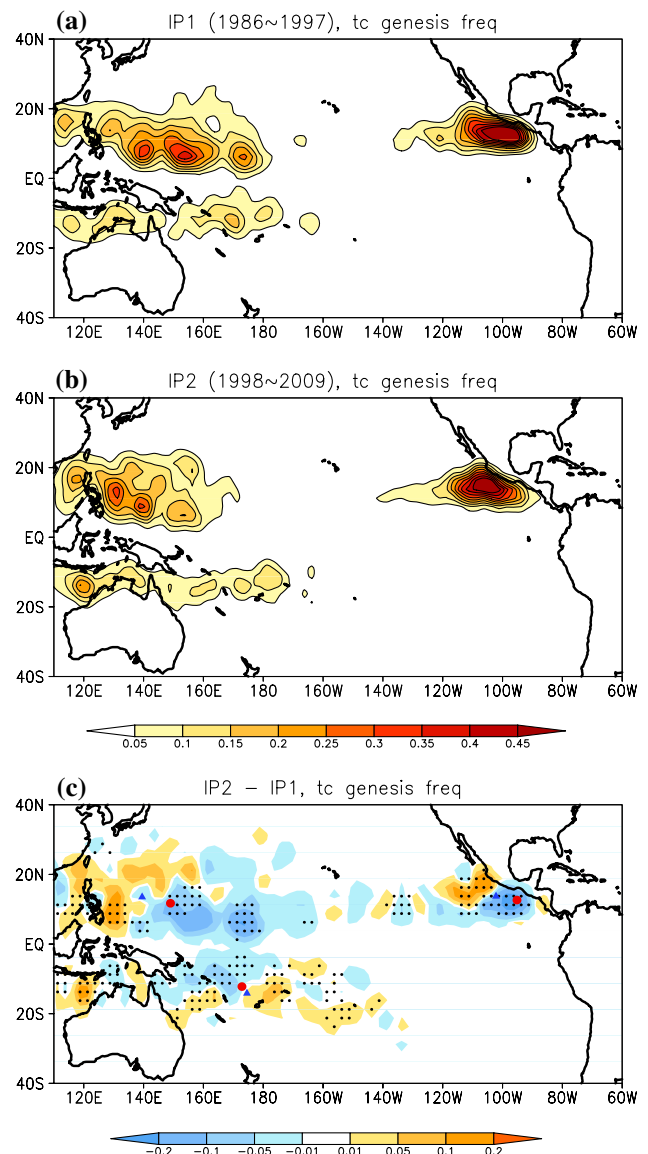
Fig. 2 Difference in TC-genesis density between the inactive period (1998–2009, IP2) and the active period (1986–1997, IP1). The symbols *red filled circle* and *blue filled triangle* denotes the mean TC-genesis position during IP1 and IP2, respectively. The *dots* indicate that the change in TC-genesis frequency was at 5 % significance level. The definition of IP1 and IP2 is based on the RSI index of TC activity shown in Fig. 1

Table 1 Comparison of the mean TC-genesis position between IP1 (1986–1997) and IP2 (1998–2009) in the Pacific Basin

Region/period	IP1 (1986–1997)	IP2 (1998–2009)
WNP	11.7°N, 149°E	13.6°N, 139.5°E
WSP	12.2°S, 173°E	14.1°S, 174.6°E
ENP	12.6°N, 95.2°W	13.8°N, 102.2°W

Figure 2 presents the horizontal distribution of the annual mean and variation of the frequency of TC genesis in the Pacific during IP1 and IP2. The most remarkable changes were the decrease in TC activity in the eastern WNP (east of 145°E) and WSP, and the increase in TC activity in the western WNP (west of 145°E). Because the decrease in the number of TCs in the eastern WNP was more pronounced than the increase in the western WNP, the total number of TCs in the WNP exhibited a decline after the late 1990s. The decrease and increase in TC activity in the eastern and western WNP, respectively, caused the mean position of TC genesis in IP2 to shift westward significantly from 149° to 140°E (Table 1). Recent studies have shown that the zonal asymmetry of local SST in the WNP (Choi et al. 2015) and the tropical tropospheric warming (Wu et al. 2015) might lead to interdecadal change in the westward shift of the mean TC genesis position in the WNP. Through numerical simulations, we demonstrated that the La Niña-like associated negative SSTA in the central Pacific might also facilitate a westward shift of the mean TC genesis position. As in the WNP, a similar westward shift of the mean TC genesis position from approximately 95°–102°W was detected in the ENP (Fig. 2c). This westward shift led to a change in TC genesis frequency, suggesting a response to global warming (Murakami et al. 2013). This indicates that the westward shift of the mean TC genesis position in the ENP was not accounted for as a specific factor. In contrast to the WNP, the interdecadal change of TC genesis frequency in the WSP between IP2 and IP1 had an N–S dipole-like structure. In other words, TC genesis frequency decreased and increased in the northern and southern WSP, respectively (Fig. 2c).

3.2 TC genesis track

Figure 3 depicts the spatial distribution of the mean TC track density in IP1 and IP2. The TC track density exhibited a remarkable decrease in the southern WNP (south of 20°N), southeastern WSP (approximately 150°–180°E), and southern ENP (south of 10°N) in IP2, among which the decrease in the southeastern WNP was the most pronounced. Conversely, an increase in TC track density was observed for particular regions, namely the region around Taiwan, the southeastern South China Sea, northeastern Australia, and the Gulf of California. The increase of TC track density in the WNP and WSP can be attributed to the substantial increase in TC genesis frequency in the eastern Philippines (120°–135°E) in IP2, owing to the westward shift of the mean TC genesis position (Fig. 2c). In addition, the westward steering flow was strengthened, experiencing a northward shift near the Philippine Sea in IP2 (Fig. 3c). This interdecadal change in steering flow, combined with the westward shift of the mean TC genesis position, led to a
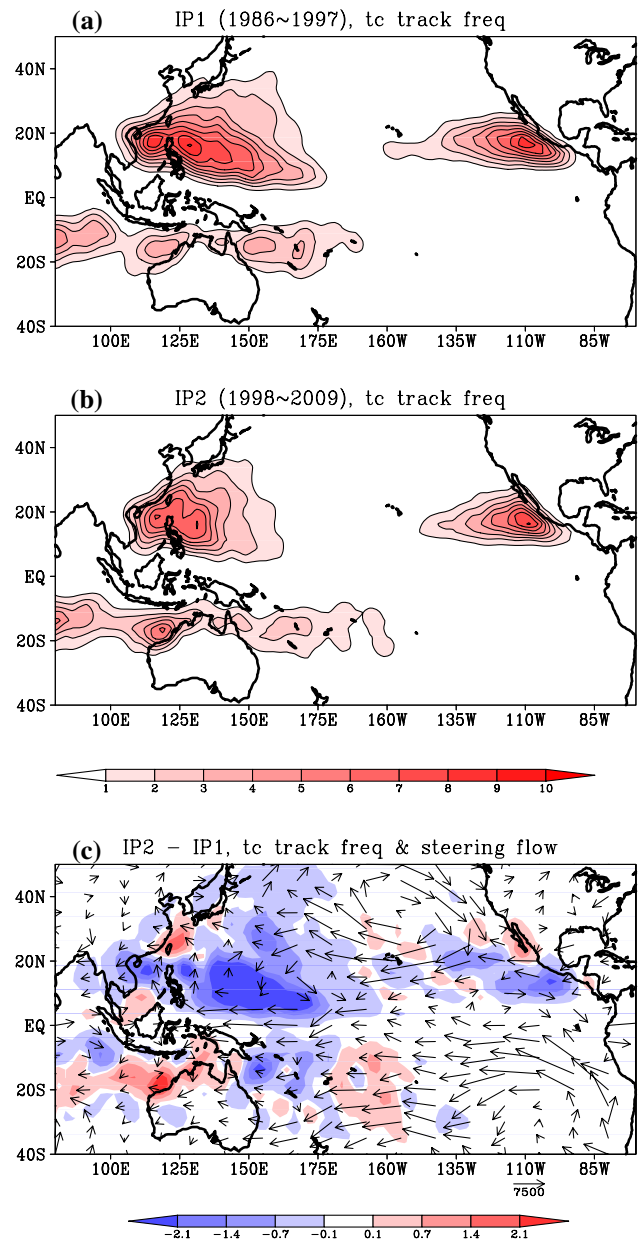
Fig. 3 Same as in the Fig. 2 except for the TC track density in **a** IP1, **b** IP2, **c** difference between IP1 and IP2. The *vectors* in **c** indicate the steering flow which is defined as the vertical integrated horizontal winds from 850 to 300 hPa

greater frequency of TC landfalls in Taiwan and southeastern China after the late 1990s.

The increase of TC track density in northern Australia can also be explained by the combined effects of the interdecadal change in steering flow and TC genesis frequency. The strengthening and westward extension of the easterly steering flow in IP2, together with the increase in TC genesis frequency off the coast of northeastern Australia (Figs. 2c and 3c), led to an increase in TC track density in northern Australia, which corresponds to one of the major

Table 2 Comparison of the annual mean of TC genesis number in various basins between IP1 (1986–1997) and IP2 (1998–2009)

TC/region	WNP	East WNP	WSP	ENP
#TC (clim)	25.7	7.3	8.7	16.8
IP1 (1986–1997)	29.1	12.8	9.9	17.8
IP2 (1998–2009)	24.2	5.3	7.8	15.5
Std (clim)	4.3	4.8	3.5	4.8
Diff (IP2–IP1)	−4.9	−7.5	−2.1	−2.3
(IP2–IP1)/IP1	−17 %	59 %	−21 %	−13 %

The definition of IP1 and IP2 is based on the clime-regime shift in the middle to late 1990s. The east WNP denotes the sub-region of the WNP at east 145°E

Table 3 Comparison of the averaged TC life cycle (unit: hour) between IP1 (1986–1997) and IP2 (1998–2009)

TC-life cycle/region	WNP	WSP	ENP
IP1 (1986–1997)	244	193	183
IP2 (1998–2009)	193	173	164
Diff (IP2–IP1)	−51	−20	−19
(IP2–IP1)/IP1	−21 %	−10 %	−10 %

TC tracks of Cluster 5 (Ramsay et al. 2012; Fig. 2), where TCs that formed in the South Solomon Sea moved westward toward the coastline of northwestern Australia. This increase in TC track density was associated with a remarkable increase in the number of severe TCs making landfall over eastern Australia after the late 1990s (Callaghan and Power 2011) (figure not shown). Another notable increase in TC track density occurred in northwestern Australia, where the TC tracks corresponded to those of Cluster 4 (Ramsay et al. 2012). The increase in TC track density was evidently caused primarily by the increase in TC genesis frequency off the coast of northwestern Australia (Fig. 2c), where rapid warming was identified after the 1980s (not shown). In the ENP, the decrease in TC track density was primarily caused by the decrease in TC genesis frequency. Thus, Figs. 2 and 3 clearly demonstrate that the interdecadal decrease in TC activity in the WNP after the late 1990s (Liu and Chan 2013; Choi et al. 2015; He et al. 2015) was part of the phenomenon of basin-scale change in TC activity in the Pacific.

A comparison of annual mean numbers of TCs in various genesis regions of the Pacific Basin between IP1 and IP2 is provided in Table 2. Decreases in TC activity in both the WNP and WSP in IP2 are evident; the annual mean number of TCs in the WNP and WSP decreased by approximately 17 and 20 %, respectively. The decrease in TC activity in the eastern WNP was partially offset by the increase in TC activity in the western WNP. Regarding the specific genesis

region of the eastern WNP, the number of TCs decreased by approximately 60 % in IP2. The TC activity in the ENP also decreased (approximately 13 %) in IP2, although the change was nonsignificant. Irrespective of TC genesis frequency, the average lifetime of TCs also experienced a remarkable decrease, particularly in the WNP, from IP1 to IP2 (Table 3). The most pronounced change occurred in the WNP, where the average TC lifetime of approximately 10 days in IP1 decreased to 8 days in IP2. A previous study suggested that this shortening of TC lifetime could have led to the recent significant decrease in the typhoon destructive potential index, despite the increase in TC intensity as a result of global warming (Lin and Chan 2015).

4 Causes of changes in TC activity

4.1 Mean-state change

Figure 4 shows the changes in the background condition between IP1 and IP2. There is an evident La Niña-like or central Pacific (CP)-type La Niña (Ashok et al. 2007) SSTA pattern, accompanied by cooling and warming in the equatorial central and western Pacific, respectively, and easterly wind anomalies (i.e., strengthened trade winds in both hemispheres) in the tropical western Pacific (Fig. 4a). In association with the K-shaped warm SST pattern in the western Pacific, an increase in relative humidity in the mid-troposphere was identified (Fig. 4b), and the increases in relative humidity along the South Pacific Convergence Zone (SPCZ) were particularly pronounced (Fig. 4b). Relative humidity is defined as q/q_s, where q and q_s denote the specific humidity and statured specific humidity, respectively. Because both q and q_s increase simultaneously in response to warming, the increase of relative humidity in the mid-troposphere is not necessarily attributable directly to SST warming. A moisture budget revealed that the increase in relative humidity at 700 hPa resulted primarily from the vertical climatological mean vapor transport caused by the anomalous vertical velocity ($-w'\nabla\overline{q}$). Specifically, the K-shaped warm SST pattern led to an anomalous vertical velocity (Fig. 5), which transported low-level humid air into the mid-troposphere, resulting in an increase in moisture at 700 hPa. Conversely, the 850 hPa vorticity exhibited a remarkable decrease in the CP in IP2 (Fig. 4c). This decrease was evidently caused by a pair of anomalous anticyclones in the CP (i.e., a Gill-type response to the CP cold SST). These anomalous anticyclones produced easterly anomalies in the equatorial CP, increasing the vertical wind shear (U_{200}–U_{850}; Fig. 4d). Matsuura et al. (2003) described the influence of dynamic conditions on interdecadal change in TC activity in the WNP, and other recent studies (e.g., Liu and Chan 2013; Hsu et al. 2014; He et al. 2015) have emphasized further that changes
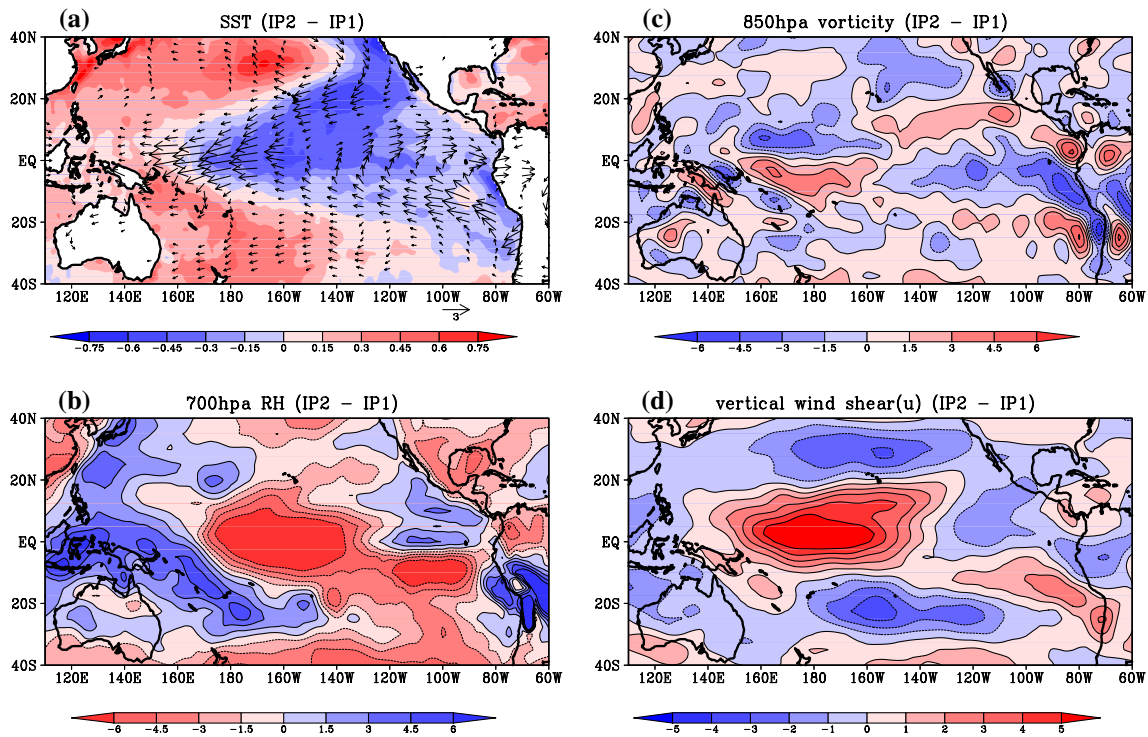
Fig. 4 The background-state difference (IP2 − IP1) associated with the decrease in TC activity in the late 1990s for the anomalous **a** SST and 850 hPa wind anomalies, **b** relative humidity at 700 hPa, **c** 850 hPa vorticity, and **d** vertical shear (200 − 850 hPa) of zonal wind
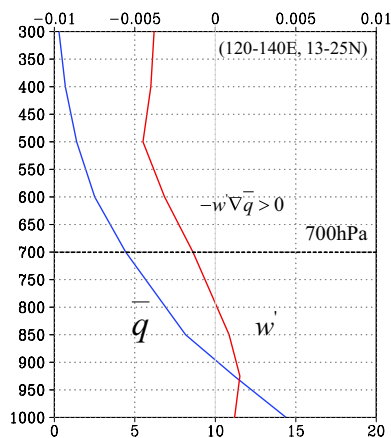

Fig. 5 The vertical profile of the climatological mean specific humidity (q) and the anomalous (IP2 − IP1) vertical velocity (w') in th west WNP (120–140°E, 13–25°N), in where the relative humidity at 700 hPa and the TC-genesis frequency experienced a remarkable increase from IP1 to IP2

in dynamics were responsible for the interdecadal decrease in the WNP after the late 1990s. The findings of this study are in accordance with these earlier studies regarding the interdecadal decrease of TC activity in the eastern WNP after the late 1990s. In addition, we demonstrated that thermodynamics, rather than dynamics, have contributed to the

interdecadal increase of TC genesis in the western WNP. The role of thermodynamics in TC activity in the South China Sea was also mentioned by Yang et al. (2012). The increase in TC genesis frequency in the northwestern ENP was primarily caused by a low-level anomalous cyclone. Additionally, the cyclone anomaly resulted in an anomalous upward motion. This transported a remarkable quantity of moist air from the boundary layer to the mid-troposphere ($-w'\nabla\overline{q} > 0$), providing a favorable environment for TC genesis. Conversely, the influence of large-scale factors on the TC activity decrease in the southeastern ENP was insignificant, a phenomenon reflected in the discrepancy between the changes in the genesis potential index (GPI) and TC genesis frequency (Figs. 2c, 6). This suggests that other physical processes (such as the intraseasonal oscillation), rather than large-scale factors, contribute substantially to the interdecadal decrease in TC activity in the southeastern ENP.

4.2 GPI analysis

Section 4.1 described the association between the change in background conditions and the change in TC activity after the late 1990s. In this section, we explain quantitatively how the mean-state change affected TC activity according to GPI analysis. The GPI (Emanuel and Nolan 2004;
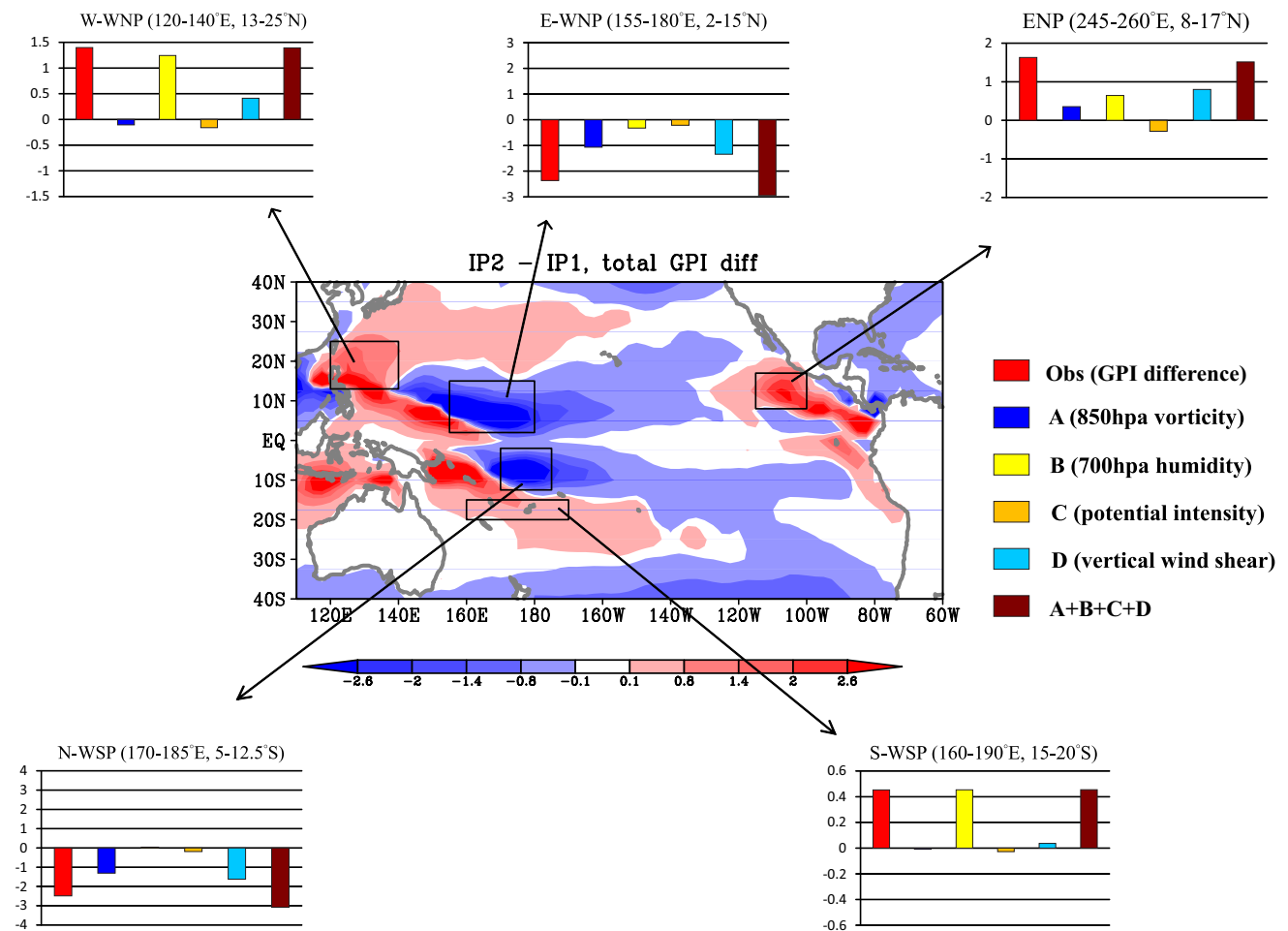
Fig. 6 a Change of the spatial distribution of GPI (Eq. 1) between IP1 and IP2 (IP2 − IP1), and the relative contribution of each term (from term *A–D*: absolute vorticity, relative humidity, potential intensity, and vertical wind shear) in the right-hand side of Eq. 1 to the total difference of GPI for the regions marked with *boxes*. Here, the contribution of each term to the total difference of GPI was calculated, following Li et al. (2013). The *box* selected for analysis was based on two criterions: (i) the change in TC-genesis frequency between IP1 and IP2 (Fig. 2c) was significant, (ii) the GPI change (Fig. 4a) well duplicates the change in TC-genesis frequency

Camargo et al. 2007) was applied to examine the specific dynamic and thermodynamic factors that caused the abrupt decline in TC activity in the late 1990s. The GPI is defined as follows:

$$GPI = \underbrace{\left|10^5 \eta\right|^{3/2}}_{(A)} \; \underbrace{\left(\frac{H}{50}\right)}_{(B)} \; \underbrace{\left(\frac{v_{pot}}{70}\right)}_{(C)} \; \underbrace{(1 + 0.1 V_{shear})^{-2}}_{(D)}, \quad (1)$$

where η denotes the absolute vorticity, H is the relative humidity at 700 hPa, v_{pot} is the potential intensity, and V_{shear} is the vertical shear of the magnitude of the horizontal wind between 200 and 850 hPa. Terms A and D are primarily related to the background dynamic conditions, whereas Terms B and C are associated with the thermodynamic conditions.

Figure 6 depicts the spatial distribution of the difference in the GPI between IP1 and IP2 (i.e., IP2 − IP1). Compared Fig. 6 with Fig. 2, the decrease in TC activity in the eastern

WNP and WSP, as well as the increase in TC activity in the western WNP and northwestern ENP, are well represented by the GPI. Considering this outcome, we examined the contributions of the individual terms. Here, the contribution of each term to the total difference in the GPI was calculated by following the suggestions of Li et al. (2013). For example, the term δA × B × C × D denotes a change caused by Term A, whereas the other terms remain unchanged; δA denotes the difference in Term A between IP1 and IP2.

Five regions (indicated by boxes in Fig. 6) where the TC genesis frequency exhibited significant change were analyzed. The analysis revealed that the abrupt decrease in the GPI in the eastern WNP during the late 1990s was caused primarily by Terms A and D, which represent changes in the background dynamics (vorticity and vertical wind shear). Conversely, the change in the thermodynamics (relative humidity at 700 hPa) contributed to the

increase in TC activity in the western WNP. In the ENP, the increase in TC activity resulted primarily from changes in vorticity (Term A) and vertical wind shear (Term D), with a partial contribution from relative humidity (Term B). In the WSP, the decrease in the northern WSP was caused primarily by changes in vorticity (Term A) and a partial contribution from vertical wind shear (Term D). Conversely, the increase of GPI in the southern WSP resulted from changes in relative humidity (Term C). Overall, the dynamic factors regulated the interdecadal decrease of the GPI in the WNP and WSP, whereas the interdecadal increase in the GPI in the western WNP (southeastern South China Sea and Philippine Sea) off the coast of northeastern Australia and the SPCZ was caused primarily by the K-shaped warm SST pattern associated with thermodynamic changes.
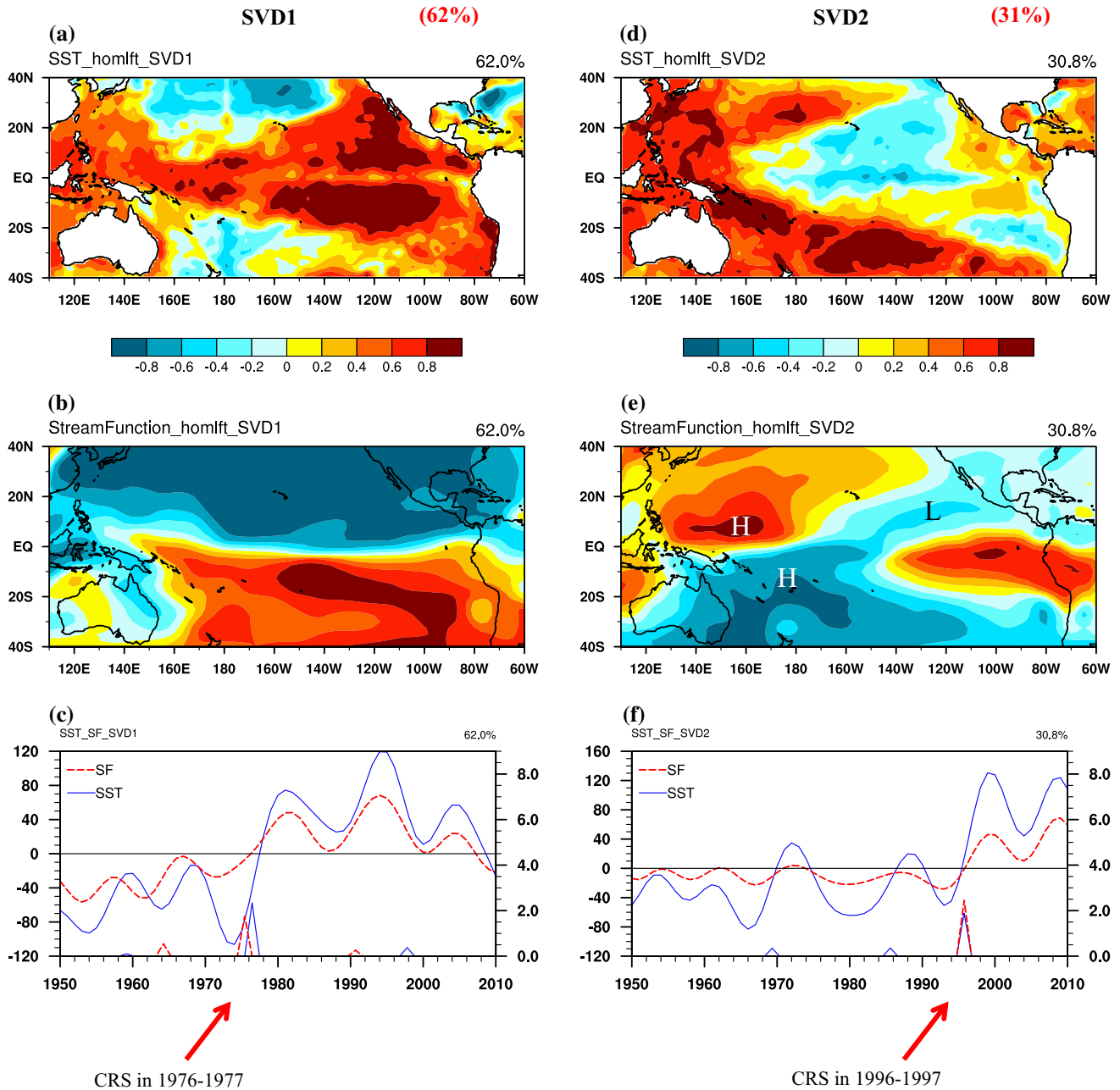
Fig. 7 (*Left*) The leading SVD pattern of interdecadal (8-year, low-pass filtered). **a** SST and **b** 850 hPa stream-function fields and **c** the corresponding principle components. The *lines* in panel (c) denote the RSI of the SST (*blue line*) and the stream function (*red line*). (*Right*) Same as in the *left* panels, except for the second SVD mode. The "H" and "L" denote the anticyclonic and cyclonic circulation anomalies, respectively

5 Influence of basin-scale CRS on the TC activity

Figure 4 shows that the abrupt change in TC activity in the Pacific after the late 1990s was associated with a La Niña-like background change. Thus, it is reasonable to consider what caused the change in background conditions. Figure 4 indicates that both the decrease in the local relative vorticity and the increase in local westerly shear were related to the anomalous low-level easterlies in the equatorial western Pacific. The anomaly of the low-level easterlies or westward shift in the vertical wind shear was caused by the change in the zonal SST gradient, which was ultimately associated with the CRS in the Pacific Basin, as discussed by Hong (2013).

Figure 7 depicts the first two leading singular value decomposition (SVD) modes of the interdecadal SST and 850 hPa stream function fields derived from Hong (2013). Whereas the first SVD mode, which has a pattern resembling the Pacific decadal oscillation (PDO) (pattern correlation coefficient: 0.95), exhibited a significant abrupt change in 1976–1977, the second SVD mode showed a significant abrupt change in 1996–1997. These changes were characterized by warming in the tropical western Pacific and cooling in the equatorial CP. Accompanying the SST pattern was a Matsuno–Gill (Gill 1980) circulation pattern, with a pair of cyclonic and anticyclonic circulation anomalies in the equatorial eastern and western Pacific, respectively (Fig. 7). The mean-state change illustrated in Fig. 5 resembles that of the SVD2 (pattern correlation coefficient: 0.91); the SSTA (with maximum observed negative SSTA in the CP) is coherent with the quadratic circulation anomalies of an anticyclone and cyclone in the western and eastern Pacific, respectively. The similarity between the spatial pattern and temporal change point suggests that the abrupt decrease in TC activity in the mid-1990s was caused by the basin-scale CRS in the Pacific during 1996–1997.

Liu and Chan (2013) argued that the significant decrease in TC activity in the WNP after the late 1990s was related to the PDO-like or interdecadal Pacific oscillation (IPO) (Meehl et al. 2013) SST change. However, the RSI calculation demonstrated that the PDO and IPO experienced a regime shift approximately in 2003 and 2005 respectively (figure not shown), lagging behind the CRS in 1996–1997 by approximately 6–8 years. This indicates that the initiation of the change in background conditions in the late 1990s resulted from SVD2, but not the PDO. Further examination revealed that the abrupt change of the SVD2-associated second principle component (PC2) in the middle to late 1990s was independent of the trend of global warming, even though that trend might have enhanced the magnitude of PC2 (figure not shown).

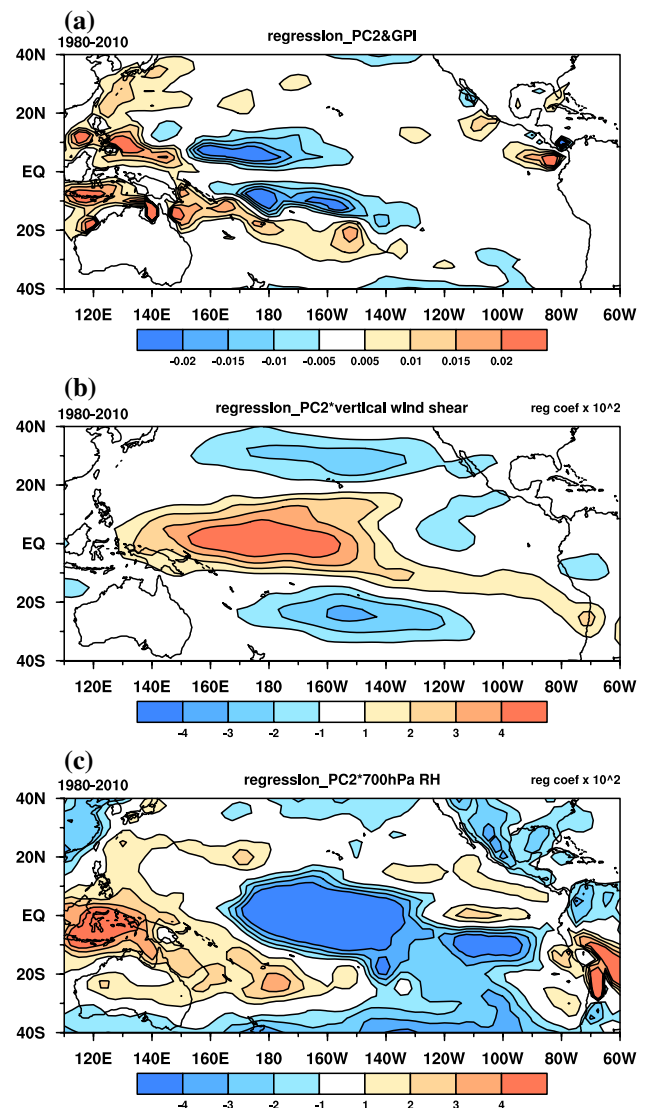The basin-wide SST underwent a significant regime shift in approximately 1996–1997. Before this regime shift,

Fig. 8 The spatial distribution of **a** GPI, **b** vertical wind shear, **c** 700 hPa relative humidity regressed on the SVD2 associated PC2

Table 4 Design of numerical experiments

Experiment	Domain	SST
CTL	Global	Climatology
PA	Pacific	Clim + SVD2 SSTA
EPA	East Pacific	Clim + east part of SVD2
WPA	West Pacific	Clim + west part of SVD2

The IP1 and IP2 denote the periods of 1986–1997 and 1998–2009, respectively

a warm SSTA appeared in the equatorial CP. In response to this warm anomaly, a Matsuno–Gill-type circulation anomaly appeared with a low-level cyclonic anomaly in the WNP. This large-scale cyclonic circulation anomaly,

together with reduced vertical shear, favored TC genesis, accounting for active TCs in the eastern WNP and the WSP in IP1. However, these anomalous oceanic and atmospheric conditions reversed after 1996–1997. The SSTA in the equatorial CP changed from positive to negative, whereas the SSTA in the equatorial western Pacific changed from negative to positive. Because of the SSTA phase change in the central equatorial Pacific, a low-level anticyclone anomaly occurred in the WNP during IP2. Meanwhile, the vertical shear increased in response to the low-level anticyclone anomaly. Both of these changes in the background state suppressed TC activity in the eastern WNP during IP2. Conversely, in response to the K-shaped warm SST pattern, an anomalous cyclone and enhanced vertical motion occurred in the western WNP. As shown in Fig. 4, these thermodynamic changes resulted in the interdecadal increase in TC genesis in the western WNP.

The influence of the basin-scale CRS on the changes in TC activity in the Pacific was demonstrated further using regression analysis. Figure 8a shows the GPI regressed on PC2. Compared with the observed GPI difference between IP1 and IP2 (Fig. 5), the negative GPI anomaly in the CP, as well as the positive GPI anomaly in the western Pacific

and ENP, were captured successfully by the regression map (pattern correlation coefficient: 0.85). Further calculation showed that the regression of the dynamics (vertical wind shear) and thermodynamics (700 hPa relative humidity) for PC2 resembled the mean-state change between IP1 and IP2 (Fig. 8b, c). These results reinforce the suggestion that the SVD2-induced La Niña-like background change resulted in the interdecadal change of TC activity in the Pacific after the late 1990s.
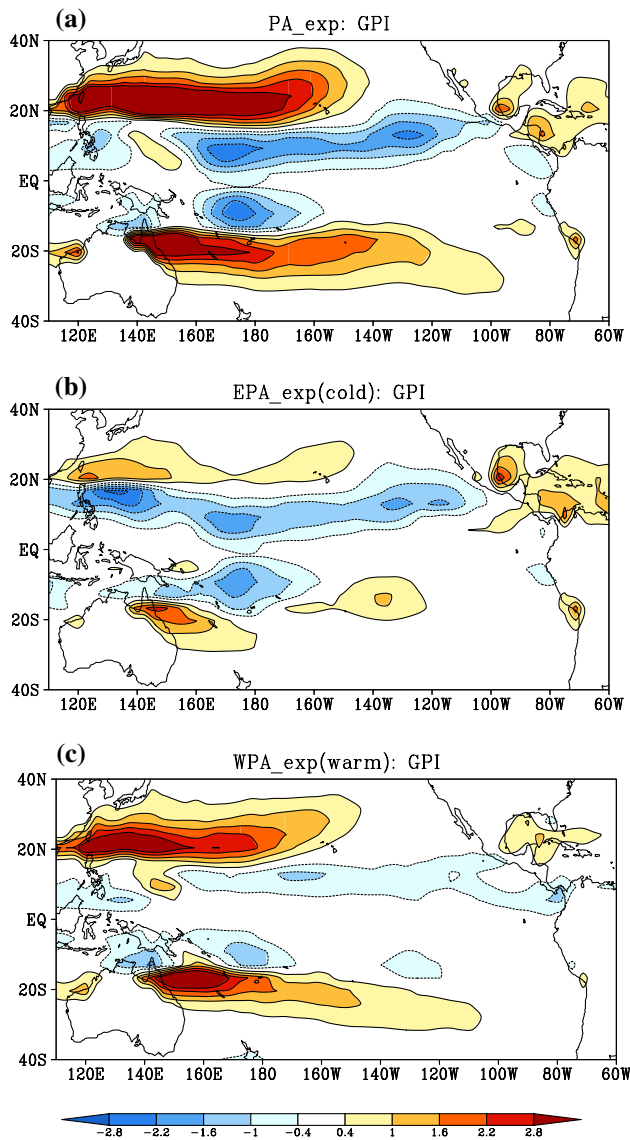
6 Numerical experiments

The regression analysis revealed that the CRS influenced the change in TC activity after the 1990s. The CRS-related SVD2 was characterized by a K-shaped positive SSTA in the western Pacific and a negative SSTA in the CP. In this section, we describe the influence of the SVD2-related SSTA on the interdecadal change in TC activity in the Pacific according to numerical experiments. The effects of the SVD2-related K-shaped warming and CP-type cooling on the GPI are also discussed.
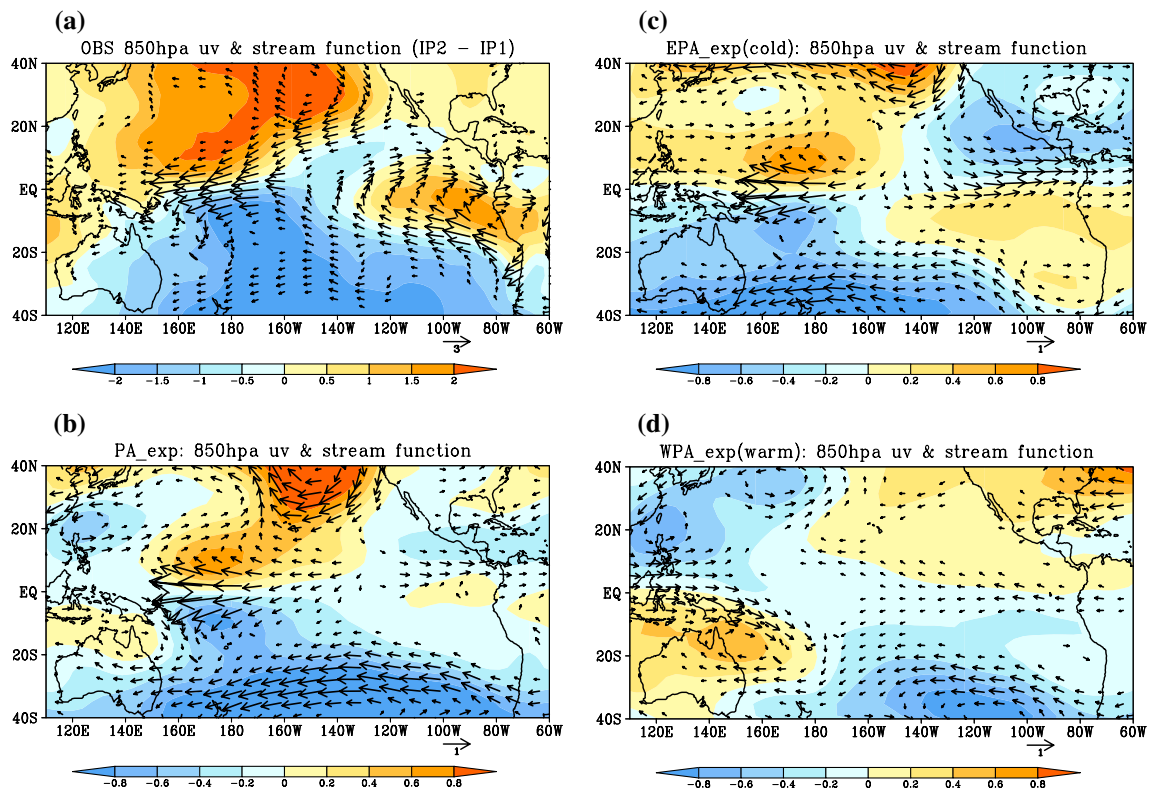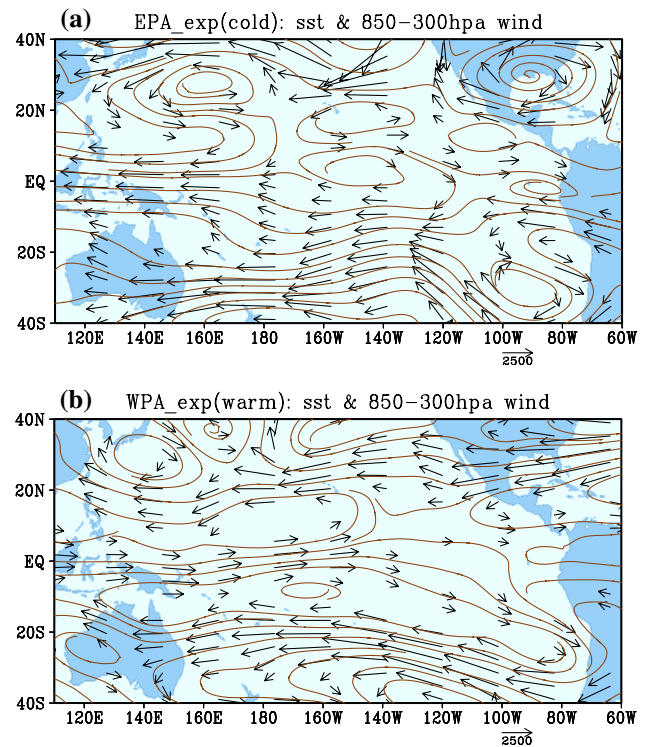

Fig. 9 Change of stream function (*shaded*) and wind at 850 hPa between the two mean states (IP2 − IP1) for **a** observation, **b–d** numerical experiments of PA, EPA, and WPA, respectively. In the PA, the model was forced by the SVD2 associated SSTA; EPA and WPA

are similar to PA except only the east and west part of the SVD2-SSTA was prescribed to the model repectively. Details of the numerical experiments are shown in Table 4

(a) PA_exp: GPI

(b) EPA_exp(cold): GPI

(c) WPA_exp(warm): GPI

Fig. 10 The simulated GPI change for the experiment of **a** PA, **b** EPA, and **c** WPA

(a) EPA_exp(cold): sst & 850−300hpa wind

(b) WPA_exp(warm): sst & 850−300hpa wind

Fig. 11 Same as in Fig. 10 except for the simulation of steering flow for **a** EPA and **b** WPA

were respectively prescribed to the model. Ten-member ensemble runs were performed for each experiment. Subsequently, each experiment was integrated for 20 years, and the 20-year mean of the SST-forced atmospheric circulations was assumed as the background mean state.

Figure 9b illustrates the anomalous 850 hPa streamfunction in response to the SSTA between IP1 and IP2. Comparing observations (Fig. 9a) revealed that the pair of anticyclonic and cyclonic circulation anomalies in the western and eastern Pacific, respectively, was replicated successfully. The anomalous cyclonic circulation in the South China Sea was also captured. The coefficient of the spatial pattern of the 850 hPa streamfunction between the observations and simulation reached 0.83. This similarity indicates that the atmospheric mean-state change during the late 1990s in the Pacific was forced by the SVD2-related SSTA.

Figure 9c, d shows the steady response of the 850 hPa streamfunction to the CP-like cooling (experiment EPA) and K-shaped warming (experiment WPA), respectively. The response revealed that the pair of low-level anticyclonic and cyclonic anomalies in the western and eastern Pacific, respectively, was forced primarily by the associated CP-like negative SSTA. Conversely, the cyclonic circulation anomaly in the South China Sea was maintained by the positive SSTA in the western Pacific. Experiment WPA (Fig. 9d) also indicated that the positive SSTA in

A general circulation atmospheric model called the simplified parameterizations primitive-equation dynamics (SPEEDY) model (Molteni 2003) was employed in the numerical experiments. The SPEEDY model is noted for its efficiency and has been used successfully in several other studies related to monsoonal dynamics (Bracco et al. 2005) and the interdecadal variation of large-scale circulations (Kucharski et al. 2006). Table 4 presents the details of the numerical experiments designed for this study. In the control experiment (CTL), the model was forced by the observed climatological monthly SST during the period 1960–2010. In the three major experiments, namely PA, WPA, and EPA, the SVD2-related SSTA, positive SSTA of SVD2 (K-shaped warming), and negative SSTA of SVD2

the western Pacific might have act to enhance the equatorial zonal SST gradient, which would be strengthen the easterly anomaly (i.e., an enhancement of the prevailing trade wind) in the CP (near 180°–160°W); consequently, the vertical wind shear in the CP was enhanced. Additionally, the enhancement of the prevailing trade winds in the Pacific would produce positive feedback for the La Niña-like SSTA (Matthew et al. 2014).

Finally, the change in the GPI in response to each SSTA (Table 3) is shown in Fig. 10b–d. Although the negative GPI in the CP was overestimated and had an eastward extension, the large-scale change in the GPI between IP1 and IP2 was accurately simulated. The success of experiment PA in simulating the GPI change again indicated that the decrease in TC activity in the Pacific Basin was caused primarily by the CRS-related SSTA. The contributions of experiments EPA and WPA to the total GPI change are shown in Fig. 10b, c respectively. The figure illustrates that the negative changes in the GPI in the eastern WNP and the WSP were caused primarily by CP-type cooling. Conversely, the positive change in the GPI in the Philippine Sea was caused by the associated K-shaped warming in the western Pacific. Additionally, the zonally distributed positive changes in the GPI in the subtropics of both hemispheres were caused primarily by the positive SSTA in the western Pacific. Figure 10c also suggests that the northward shift of the TC genesis mean position in the WNP was a result of the K-shaped warming. Thus, the numerical experiments confirmed the findings of the regression analysis and demonstrated that the large-scale decline in TC activity in the eastern WNP and northern WSP after the late 1990s was attributed to CP-type cooling. Nevertheless, the increase in TC activity in the western WNP and southern WSP (distributed along the SPCZ) was caused primarily by K-shaped warming of the SST in the western Pacific.

7 Conclusions and discussion

This study examined whether the abrupt change in TC activity in the Pacific in the middle to late 1990s was caused by changes in the background conditions induced by the basin-scale CRS in the middle to late 1990s, and how the basin-scale CRS affected the interdecadal change in TC activity in the Pacific through GPI analysis and numerical experiments. It has been established that a basin-scale CRS in the Pacific and an abrupt change in TC activity in various genesis regions, including the WNP, WSP, and ENP, occurred simultaneously in the middle to late 1990s. The simultaneous concurrence of these two abrupt changes suggests that they were possibly related. We hypothesized that the abrupt change in TC activity in the Pacific Basin during the late 1990s was primarily caused by the CRS-induced

La Niña-like SSTA pattern. The basin-scale CRS after the late 1990s induced large-scale changes in both oceanic and atmospheric conditions, which led to the abrupt decline in TC genesis in the WNP and a significant change in TC activity in the ENP and WSP. The main results of this study are summarized as follows:

1. Significant changes in TC activity were identified during the late 1990s in various genesis regions of the Pacific. These included a marked decrease in TC activity in the eastern WNP and the WSP, and an increase in TC activity in the Philippine Sea and southeastern South China Sea. Irrespective of the interdecadal change in the number of TCs, the mean TC genesis position in the WNP and ENP also exhibited a remarkable westward shift after the late 1990s.

2. A GPI diagnosis revealed that the major large-scale factors that caused the decrease in TC activity in the eastern WNP and northern WSP were related to changes in the dynamic conditions (i.e., a decrease in low-level vorticity and an increase in vertical wind shear). Conversely, the change in thermodynamic conditions (i.e., increase in 700 hPa relative humidity) contributed to the abrupt increase in TC activity in the western WNP and southern WSP. The increase in 700 hPa relative humidity was caused by the enhancement of vertical climatological mean vapor transport by the anomalous vertical velocity produced by the K-shaped warming. Both the thermodynamic and the dynamic conditions contributed to the change of TC activity in the ENP.

3. Observations revealed that the changes in the background conditions from IP1 to IP2 were caused primarily by the basin-scale CRS during the middle to late 1990s. A GPI regression in the CRS-related PC2 confirmed that the CRS could have led to the interdecadal change in TC activity in the Pacific in the late 1990s.

4. Numerical experiments showed that the interdecadal decline in TC genesis in the eastern WNP and northern WSP was primarily attributable to the CRS-related CP-type cooling. However, the CRS-related K-shaped warming in the western Pacific contributed to the interdecadal increase in TC genesis in the western WNP and southern WSP.

It has been identified that an abrupt change occurred in TC activity in the various genesis regions of the Pacific during the late 1990s. The interdecadal decrease in TC activity in the WNP during the late 1990s has been widely reported in recent studies (Liu and Chan 2013; Hsu et al. 2014; Choi et al. 2015; He et al. 2015). However, in this paper, a new interpretation of this interdecadal change is proposed. Furthermore, several new scientific findings are illustrated, such as the decrease in TC genesis frequency in the northern WSP, the physical

processes leading to the increase in TC genesis frequency in the western WNP, and the increase of TC landfalls over Taiwan and northeastern Australia. Here, we assumed that the abrupt change in TC activity in the WNP during the late 1990s was part of the phenomenon of basin-scale change in TC activity in the Pacific (i.e., a decrease in TC activity in the eastern WNP and northern WSP, an increase in the northwestern WNP, and changes in the mean position of TC genesis in the WNP and ENP). We demonstrated that the interdecadal change in TC activity in the Pacific during the late 1990s was forced by the La Niña-like SSTA pattern caused by the CRS in the Pacific during the middle to late 1990s. The numerical experiments further indicated that the declines in TC activity in the eastern WNP and northern WSP were attributable to the negative SSTA in the CP. Conversely, the increases in TC activity in the western WNP and southern WSP were caused by the K-shaped warm SST pattern in the western Pacific. Although the number of TCs in the ENP does not show significant interdecadal change, the mean TC genesis position shifted westward significantly from 95° to 102°W during IP2. The numerical experiments also indicated that the westward shift of the mean TC genesis position in the ENP and WNP was caused primarily by the large-scale low-level cyclonic and anticyclonic circulation anomalies in the ENP and WNP, respectively.

Figure 2 shows that the mean positions of TC genesis in WNP and ENP experienced a significant westward shift from IP1 to IP2. The major reason the change in TC tracks in the ENP did not exhibit a westward shift as detected in the WNP (Fig. 3a, b) is that the anomalous low-level cyclone resulting from the La Niña-associated negative SSTAs in the eastern Pacific (Fig. 9c) weakened the climatologically westward steering flow (Fig. 11a), substantially preventing the westward movement of TC tracks in the ENP.

Notably, the westward shift of the mean TC genesis position in the WNP was accompanied by an increase in TC activity in the western WNP and southeastern South China Sea (e.g., Yang et al. 2012). Previous studies have shown that the increase in TC activity in the western WNP could lead to a significant increase in TC landfalls in Taiwan (Tu et al. 2011; He et al. 2015). Irrespective of the increase in TC genesis frequency, our study showed that the modulation effect of the CRS on the steering flow (i.e., westward extension and northward curving near the Philippine Sea) also contributed substantially to the increase in TC landfalls in Taiwan after the late 1990s. The numerical experiments showed that the increase in TC genesis frequency in the western WNP resulted from the K-shaped warm SST induced thermodynamic changes. In other words, the K-shaped warm SST created wet conditions in the midtroposphere via the anomalous vertical vapor transport (Figs. 6 and 10), which favored TC genesis. Furthermore,

the K-shaped warm SST modified the steering flow (westerly), causing it to extend substantially westward (Fig. 11b). The numerical experiments showed consistency with the observational analysis, indicating that the modulation effect of the K-shaped warm SST on the steering flows and TC genesis frequency might have led to the significant increase in TC landfalls in Taiwan and southeastern China after the late 1990s (Figs. 3 c and 11b).

Another notable finding concerns the increase in TC landfalls in northeastern and northwestern Australia after the late 1990s. Although the SVD analysis (Fig. 7) showed that the interdecadal change of SVD2 was independent of global warming, the warming trend enhanced the magnitude of PC2 by approximately 20 %. The increase in TC genesis in the WSP occurred off the coast of northeastern and northwestern Australia, where rapid warming after the 1980s was identified (not shown). Because the increase in TC genesis frequency in these regions was caused primarily by changes in the thermodynamics (i.e., warm SSTs), the question of whether TC landfalls in northeastern and northwestern Australia will become more frequent in response to global warming is under investigation.

In this study, we focused on the influence of the CRS on the interdecadal change in TC activity in the Pacific Basin. The impact of the CRS during 1976–1977 (Fig. 7, left panels) was not considered. Figure 1c illustrates that the number of TCs in the ENP also increased significantly during 1976–1977. However, this interdecadal change was not observed in either the WNP or WSP (Fig. 1b, c). Regarding the lack of impact of the CRS on TC activity in the WNP for 1976–1977, Fig. 7 shows that PC1 and PC2 were out of phase during the period of inactive TC genesis during 1976–1984, whereas they were in phase during 1998–2011. This observation suggests that the large-scale environmental change associated with SVD1 in 1976–1977 was partially offset by the effect of SVD2. In addition to the large-scale factors, the interdecadal variation in TC activity in the WNP was also affected by other processes, such as intraseasonal oscillations (Hsu et al. 2008; Kim et al. 2008; Ha et al. 2014), which cannot be measured using the interdecadal time scale. The interdecadal change in TC activity in other periods, such as the increase in TC activity in the ENP during 1976–1977 and the increase in TC activity in the WNP during the late 1980s, might be attributable to other processes not currently under investigation.

References

Ashok K, Behera SK, Rao SA, Weng H, Yamagata T (2007) El Niño Modoki and its possible teleconnection. J Geophys Res 112:C11007. doi:10.1029/2006JC003798

Bracco A, Kucharski F, Molteni F, Hazeleger W, Severijns C (2005) Internal and forced modes of variability in the Indian Ocean. Geophys Res Lett 32:L12707

Callaghan J, Power SB (2011) Variability and decline in the number of severe tropical cyclones making land-fall over eastern Australia since the late nineteenth century. Clim Dyn 37:647–662

Camargo SJ, Sobel AH (2005) Western North Pacific tropical cyclone intensity and ENSO. J Clim 18:2996–3006

Camargo SJ, Emanuel KA, Sobel AH (2007) Use of a genesis potential index to diagnose ENSO effects on tropical cyclone genesis. J Clim 20:4819–4834

Chan JCL (2000) Tropical cyclone activity over the western North Pacific associated with El Niño and La Niña events. J Clim 13:2960–2972

Chan JCL (2005) Interannual and interdecadal variations of tropical cyclone activity over the western North Pacific. Meteorol Atmos Phys 89:143–152. doi:10.1007/s00703-005-0126-y

Chia HH, Ropelewski CF (2002) The interannual variability in the genesis location of tropical cyclones in the northwest Pacific. J Clim 15:2934–2944

Choi Y, Ha KJ, Ho CH, Chung CE (2015) Interdecadal change in typhoon genesis condition over the western North Pacific. Clim Dyn 45:3243–3255

Emanuel KA, Nolan DS (2004) Tropical cyclone activity and global climate. Preprints, 26th conference on hurricanes and tropical meteorology, Miami, FL, Am Meteorol Soc, pp 240–241

England MH, McGregor S, Spence P, Meehl GA, Timmermann A, Cai W, Gupta AS, McPhaden MJ, Purich A, Santoso A (2014) Recent intensification of wind-driven circulation in the Pacific and the ongoing warming hiatus. Nat Clim Change 4:222–227. doi:10.1038/nclimate2106

Gill AE (1980) Some simple solutions for heat-induced tropical circulation. Quart J Roy Meteorol Soc 106:447–462

Ha Y, Zhong Z, Sun Y, Lu W (2014) Decadal change of South China Sea tropical cyclone activity in mid-1990s and its possible linkage with intraseasonal variability. J Geophys Res 119:5331–5344. doi:10.1002/2013JD021286

He H, Yang J, Gong D, Mao R, Wang Y, Gao M (2015) Decadal changes in tropical cyclone activity over the western North Pacific in the late 1990s. Clim Dyn 45:3317–3329. doi:10.1007/s00382-015-2541-1

Hong C-C, Wu Y-K, Li T, Chang C-C (2013) The climate regime shift in Pacific during 1996/1997. doi:10.1007/s00382-013-1867-9

Hsu H-H, Chen Y-L, Lo A-K, Hung C-H, Kau W-S, Wu C-C (2008) Intraseasonal oscillation–tropical cyclone coupling in the Western North Pacific during the 2004 typhoon season. In: Liou KN, Chou MD (eds) Recent progress in atmospheric sciences: applications to the Asia-Pacific region. World Scientific, Singapore, pp 49–65

Hsu P-C, Chu P-S, Murakami H, Zhao X (2014) An abrupt decrease in the late-season typhoon activity over the Western North Pacific. J Clim 27:4296–4312. doi:10.1175/JCLI-D-13-00417.1

Kalnay E et al (1996) The NCEP/NCAR 40-year reanalysis project. Bull Am Meteorol Soc 77:437–471

Kim JH, Ho CH, Kim HS, Sui CH, Park SK (2008) Systematic variation of summertime tropical cyclone activity in the Western North Pacific in relation to the Madden–Julian oscillation. J Clim 21:1171–1191. doi:10.1175/2007JCLI1493.1

Knapp KR, Kruk MC, Levinson DH, Diamond HJ, Neumann CJ (2010) The international best track archive for climate stewardship (IBTrACS): unifying tropical cyclone best track data. Bull Am Meteorol Soc 91:363–376. doi:10.1175/2009BAMS2755.1

Kucharski F, Molteni F, Bracco A (2006) Decadal interactions between the western tropical Pacific and the North Atlantic oscillation. Clim Dyn 26:79–91

Li T (2012) Synoptic and climatic aspects of tropical cyclogenesis in Western North Pacific. In: Oouchi K, Fudeyasu H (eds) Cyclones: formation, triggers and control, chap 3. Nova Science Publishers, Inc., pp 61–94

Li Z, Yu W, Li T, Murty VSN, Tangang F (2013) Bimodal character of cyclone climatology in Bay of Bengal modulated by monsoon seasonal cycle. J Clim 26(3):1033–1046

Lin II, Chan JCL (2015) Recent decrease in typhoon destructive potential and global warming implications. Nat Commun 6:7182

Liu KS, Chan JCL (2013) Inactive period of western North Pacific tropical cyclone activity in 1998–2011. J Clim 26:2614–2630

Lupo AR (2011) The interannual and interdecadal variability in hurricane activity, recent hurricane research—climate, dynamics, and societal impacts. In: Prof. Anthony Lupo (ed), ISBN: 978-953-307-238-8, InTech. http://www.intechopen.com/books/recent-hurricane-research-climate-dynamics-and-societal-impacts/the-interannual-and-interdecadal-variability-in-hurricane-activity

Matsuura T, Yumoto M, Iizuka S (2003) A mechanism of interdecadal variability of tropical cyclone activity over the western North Pacific. Clim Dyn 21:105–117. doi:10.1007/s00382-003-0327-3

Meehl GA, Hu A, Arblaster JM, Fasullo JY, Trenberth KE (2013) Externally forced and internally generated decadal climate variability associated with the Interdecadal Pacific oscillation. J Clim 26:7298–7310

Molteni F (2003) Atmospheric simulations using a GCM with simplified physical parametrizations. I. Model climatology and variability in multi-decadal experiments. Clim Dyn 20:175–191. doi:10.1007/s00382-002-0268-2

Murakami H, Wang B, Li T, Kitoh A (2013) Projected increase in tropical cyclones near Hawaii. Nat Clim Change 3:749–754. doi:10.1038/nclimate1890

Ramsay HA, Camargo SJ, Kim D (2012) Cluster analysis of tropical cyclone tracks in the Southern Hemisphere. Clim Dyn 39:897–917

Rayner NA, Parker DE, Horton EB, Folland CK, Alexander LV, Rowell DP, Kent EC, Kaplan A (2003) Global analyses of sea surface temperature, sea ice, and night marine air temperature since the late nineteenth century. J Geophys Res 108:4407. doi:10.1029/2002JD002670

Rodionov SN (2004) A sequential algorithm for testing climate regime shifts. Geophys Res Lett 31:L09204. doi:10.1029/2004GL019448

Tu J-Y, Chou C, Huang P, Huang R-H (2011) An abrupt increase of intense typhoons over the western North Pacific in early summer. Environ Res Lett 6:034013. doi:10.1088/1748-9326/6/3/034013

Wang B, Chan JCL (2002) How strong ENSO events affect tropical storm activity over the western North Pacific. J Clim 15:16431658

Wu L, Wang C, Wang B (2015) Westward shift of western North Pacific tropical cyclogenesis. Geophys Res Lett 42:1537–1542

Yang L, Du Y, Xie S, Wang D (2012) An interdecadal change of tropical cyclone activity in the South China Sea in the early 1990s. Chin J Oceanol Limnol 30:953–959